

HSM2014-14025

**TRAJECTORIES IN LASER MACHINING CERAMICS:
THERMAL MODEL TO CONTROL MATERIAL REMOVE RATE**A. Demarbaix^{1*}, F. Ducobu¹, E. Rivière-Lorphèvre¹, E. Filippi¹, F. Petit², N. Preux²¹University of Mons, Faculty of Engineering, Machine Design and Production Engineering Department,
Mons, Belgium²Environmental Materials Research Association, R&D Support, Mons, Belgium

*Corresponding author; e-mail: anthonin.demarbaix@umons.ac.be

Abstract

Ceramic conventional machining faces a lot of practical difficulty due to its mechanical properties leading to high cutting forces, fast tool wear and problems to achieve given tolerances. Laser machining is an attractive alternative to conventional machining techniques because this technology is a non-contact, non-abrasive one which eliminates tool wear, cutting forces, vibration. However, the disadvantage of this method is to master material removal rate. In fact, the appearance of hot spot could cause an uncontrolled material removal rate. Results of these investigations have compared several paths to predict the better trajectory allowed for a steady rate.

Keywords:

Laser machining; ceramics; trajectories; thermal model; paths; machining strategy

1 INTRODUCTION

Yttria-stabilized tetragonal zirconia polycrystalline (Y-TZP) finds a good alternative application in the dental restoration because of its biocompatibility and attractive mechanical properties [Filsler 2001]. Y-TZP have superior strength, fracture toughness against other dental ceramics because of its transformation toughening mechanism [Denry 2008].

The conventional machining of Y-TZP is very difficult due to its mechanical properties leading to high cutting forces (yield strength), fast tool wear (hardness) and problems to achieve desired tolerances (brittle behavior).

The laser machining is a good alternative because this type of machining is a non-contact tool process and non-abrasive [Vora 2013].

Laser machining is a method allowing building of a ceramic piece layer by layer by removing material. However, the problem of this method is to master material removal rate. In fact, the thermal effects play an important role during laser machining because of appearance of hot spots that could cause an uncontrolled material removal rate. These hot spots can cause excessive removal of material on one layer, the next layer will be affected. This cumulative effect can damage and weaken the ceramic part.

The object of this article is to compare several paths to predict the better trajectory allowed for a steady rate.

To do this, the heating process with laser is modelled using the finite element method. A thermal model of a moving heat source is developed with the software ABAQUS v6.11. This simplified model is a first step of the laser machining simulation. Although hypothesis are made for this first approach (no crater formation, material properties independent of temperature). The power output of the laser, its spot diameter and the scanning speed are implemented in this model. This one will be validated with analytical model which is considered as reference.

This paper presents three strategies: Zig path, Zig-Zag path and contour parallel path. The reference laser machining strategy is unidirectional (Zig). These trajectories are compared using numerical simulation results of a heat moving source on a pocket square.

Then an island will be added the centre of the pocket. The contour parallel strategy and the reference strategy will be compared. The island size will varied to study the island size influence.

These trajectories are compared in term of heating time and temperature maps.

These maps allowed to localize hot spots and to choose the best strategy.

2 HEAT MOVING SOURCE

First, an analytical approach of the thermal exchange between a material block and a heat source will be exposed.

Then, a numerical model will be developed to represent this thermal exchange.

The numerical results of the thermal model will be compared with the analytical solution.

2.1 Analytical model

The differential equation of heat transfer is [Carslaw 1959]:

$$\frac{\partial^2 T}{\partial x^2} + \frac{\partial^2 T}{\partial y^2} + \frac{\partial^2 T}{\partial z^2} = \frac{1}{\alpha} \frac{\partial T}{\partial t} \tag{1}$$

T is the temperature, α is the diffusivity (m^2/s), t is the time (s) and x, y, z is the coordinate system (m).

A moving heat source has been performed to simulate laser welding process. Rosenthal has proposed a solution for moving point heat source. This solution is based on a quasi stationary solution. A local coordinate system (ξ, y', z') moving with a speed v is defined against a global coordinate system fix (x, y, z). These coordinates system are described in Fig. 1 [Darmadi 2011].

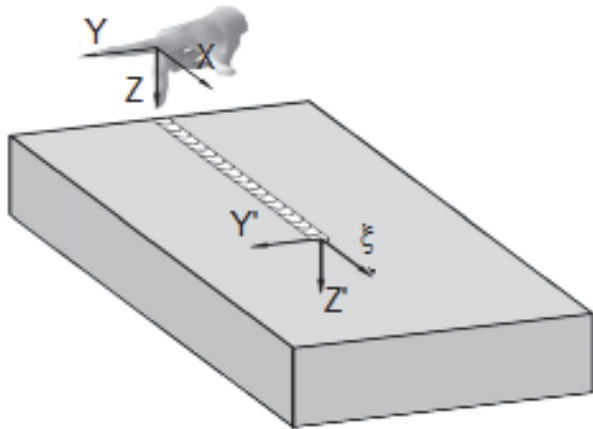


Fig. 1: Fixed coordinate system and moving coordinate system adapted of [Darmadi 2011]

With asymmetric function along line parallel to ξ and symmetric function along y and z , a final solution is proposed by Rosenthal for moving point heat source for semi-infinite solid:

$$T = T_{\infty} + \frac{Q}{2\pi\lambda r} e^{\frac{-v}{2\alpha}(r+\xi)} \tag{2}$$

T_{∞} is the ambient temperature, λ is the conductivity (W/mK), α is the diffusivity (m^2/s) and r is the distance between the heat source point and the target point.

2.2 Laser modelling

The laser is not continuous wave source but a multipulse source [Vora 2013]. In the pulse mode, the multiple laser pulses are projected repeatedly on the material with a short pulse width. The surface temperature increases during the application of a pulse followed by a cooling until the next pulse (see Fig. 2).

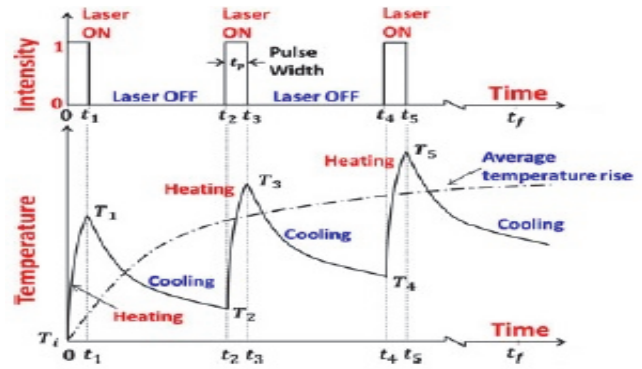


Fig. 2: Schematic of laser machining processes: temperature as function of time [Vora 2013]

Several process parameters may be varied to determine the optimum values for the process (repetition rate, scan velocity...). The pulsation distance, illustrated in Fig. 3 can be obtained from the repetition rate, scanning speed and spot diameter [Kaldos 2004]. The degree of overlap, Ud (%), is defined to determine the distance between each pulses as:

$$Ud = [1 - v(f_p D)^{-1}] 100\% \tag{3}$$

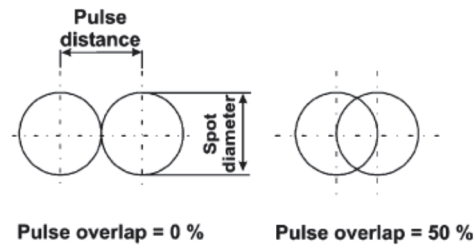


Fig. 3: Pulse distance and overlap [Kaldos 2004]

with the repetition rate f_p (kHz), the laser spot diameter D (μm) and the scan velocity v (mm/s). The Fig. 4 illustrates an example with a spot diameter of $45 \mu m$.

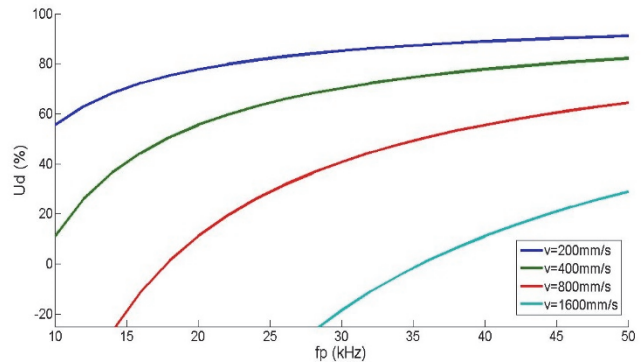


Fig. 4: Overlap behavior at a spot diameter of $45 \mu m$

The surface finishing is essentially influenced by the pulse overlap. In fact, the surface finishing essentially depends from repetition rate and scan velocity [Kaldos 2004].

2.3 Numerical model

Temperature field is determined using "Heat transfer" function available within finite element analysis of the software Abaqus v6.11. In this model, the thermo-physical properties (density, conductivity and specific heat) do not depend on temperature. Abaqus thermal analysis is based on the conservation energy law and Fourier's law. The field temperature is expressed as [Piekarska 2010]:

$$\int_V \rho U \delta \dot{T} dV + \int_V \frac{\partial \delta T}{\partial x} \left(\lambda \frac{\delta T}{\partial x} \right) dV = \int_V \delta T q_v dV + \int_S \delta T q_s dS \quad (4)$$

With U internal energy (J), q_v is a laser beam heat source (W/m^3) and q_s is a heat flux toward element surface (W/m^2).

The heat flux is applied on a circular surface with diameter of $45 \mu m$ corresponding to the laser spot but it is transformed in a square equivalent surface (see Fig. 5) in order to correspond the rectangular mesh. The equivalent side of the square is $50 \mu m$.

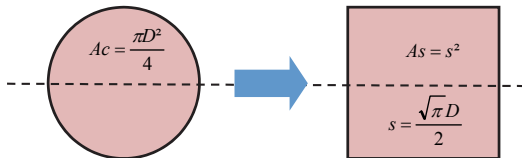


Fig. 5: Equivalent surface

The model developed is a Y-TZP bloc, $3450 \times 450 \times 200 \mu m$, a heat source travelling on it along X on 3 mm. The thermo-physical proprieties are $\lambda = 2.2 W/mK$, $\rho = 6050 kg/m^3$ and $c_p = 550 J/kg K$. The laser type is a Nd:YAG and its parameters are the power of 20W, a scanning speed of 800 mm/s and repetition rate of 18 kHz (The overlap is 0%). The condition initial is ambient temperature to $20^\circ C$.

The field temperature result is shown in Fig. 6.

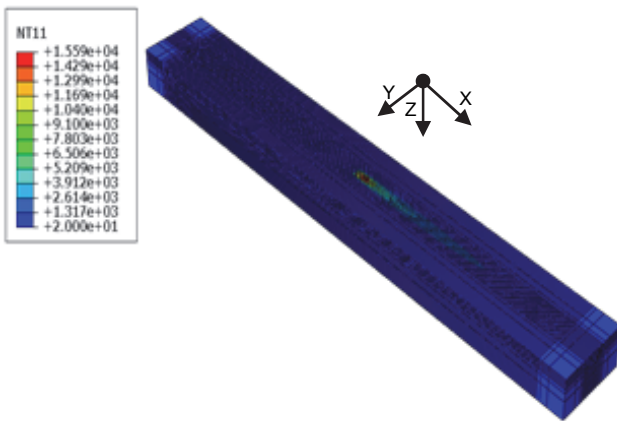


Fig. 6: Field temperature (in $^\circ C$) at a time of 2 ms with rectangular mesh of $5 \mu m$ and number elements 324786

2.4 Discussion

Fig. 7 shows the temperature evolution at node localized at $37.5 \mu m$ depth on symmetric axis in middle path as a function of time. This target nodes was chosen arbitrarily. This graphic allows to compare analytical and numerical solutions.

The numerical and analytic of Rosenthal curves are similar except at the peak.

The Rosenthal solution is a solution for moving heat source point. While our model gives a solution for a moving uniform surface heat source. This variance could explain the peak difference [Darmadi 2011]. This may as a result of the use non uniform meshes too.

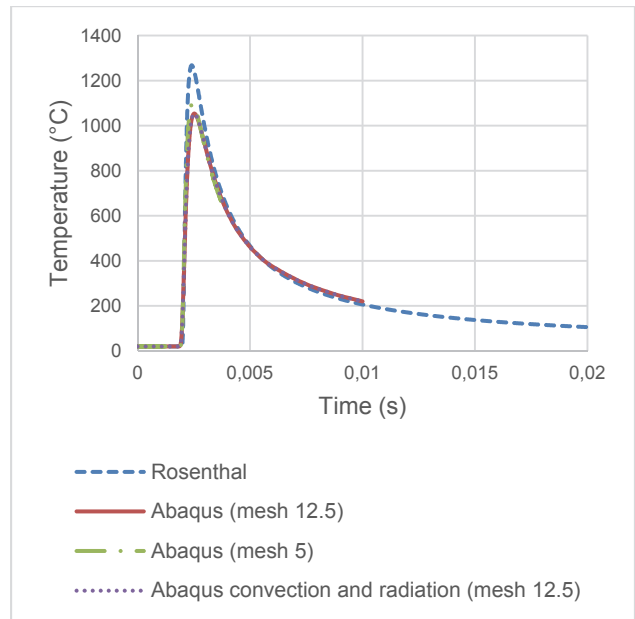


Fig. 7: Comparison of numerical and analytical solutions at a point located at 1.5 mm (along X) from start and $37.5 \mu m$ depth along Z and at the middle of the blank along Y

The convection and radiation interventions do not influence. They will be negligible in next models to win calculation times (four times more fast).

The mesh of $5 \mu m$ is nearest of the analytical solution but calculation time is raised (see Tab.1). Indeed, the calculation time is 49 times more important than this one with a mesh of $25 \mu m$.

Tab. 1: Mesh influence on the calculation time

	Number of elements	Calculation time factor
Mesh 5 μm	324786	49
Mesh 10 μm	53088	8
Mesh 25 μm	7800	1

The mesh of $10 \mu m$ is chosen to compare the different strategies. In fact, the comparison is realized against numerical results obtained of the reference strategy.

Unfortunately the literature does not permits to compare these numerical results with the experimental experiments on the 3D laser machining.

3 STRATEGIES COMPARISON METHOD

3.1 Model

A model has been developed to compare several trajectories. This model is a Y-TZP bloc of $2 \times 2 \times 0.5 mm$ with a heat source who scans the upper surface on a square of $1 \times 1 mm$. The thermo-physical are identical to the §2.3 (see Fig. 8). The scanning speed of laser on is 800 mm/s without overlap (0%) and of laser off is 5 m/s. The power output is 20 W with spot square equivalent with $50 \mu m$ by side and a repetition rate of 18 kHz (cf. §2.3).

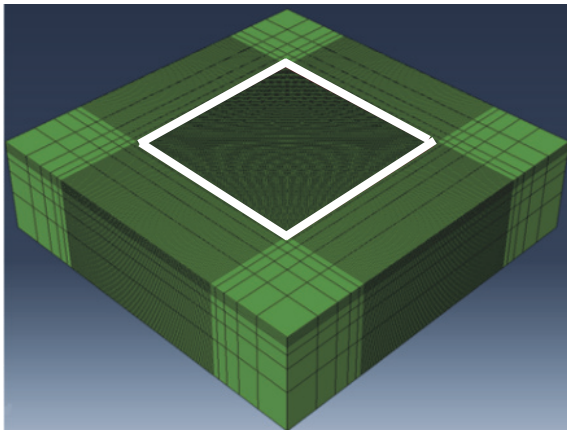


Fig. 8: FEM model to compare several trajectories with number element type of 121104 (with heating zone in wit)

The meshes are of 10 μm on the surface in interaction with the laser (see §2.4).

Several strategies are studied: Zig, Zig-Zag and contour parallel (see Tab. 2). The usual strategy in laser machining is the Zig trajectory [Heyl 2001]: a layer is machined unidirectional in one direction and the next layer is machined in perpendicular direction to the previous one, as shown in Fig. 9.

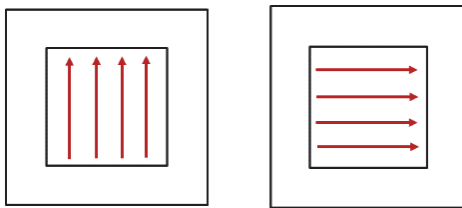


Fig. 9: Reference strategy (Zig)

The Zig-Zag and contour parallel strategies are compared with this reference.

Tab. 2: Strategies laser machining

Strategies	ZIG	ZIG – ZAG	CONTOUR
Trajectories			

3.2 Method

The method developed to compare the strategies is:

- First, the model with a machining strategy is numerically solved within the finite element software.
- Then, a path crossing the pocket is defined to record temperature evolution to nodes located on the path.
- These recordings allow to create a temperature map and compare the strategies.
- These maps are simplified in the two-dimensional graphic to improve the comparison.

The graphics for each strategy are superposed to compare the hot spots and machining time.

Paths definition

Three paths are chosen: Path 1 crosses to the pocket middle, path 3 is perpendicular and it crosses also to the

middle, path 2 is parallel to the path 1 and it crosses to the square corner (bifurcation).

These paths are strategic paths to take into account the different meetings between paths and the laser: the laser travels one path along (path 3), it crosses several times other path (path 1) and it crosses to the direction change (path 2).

These paths will be used to for recording temperature evolution of nodes localized on the path.

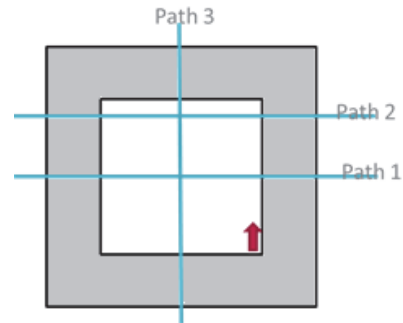


Fig. 10: Path definition

The temperature evolution of 101 equidistant nodes will be recorded.

Temperature map

The temperature map is generated from these records (Fig. 11): the time on the X axis, the length path on the Y axis and the temperature is on the Z axis. These maps are allow to visually compare hot spots between the trajectories.

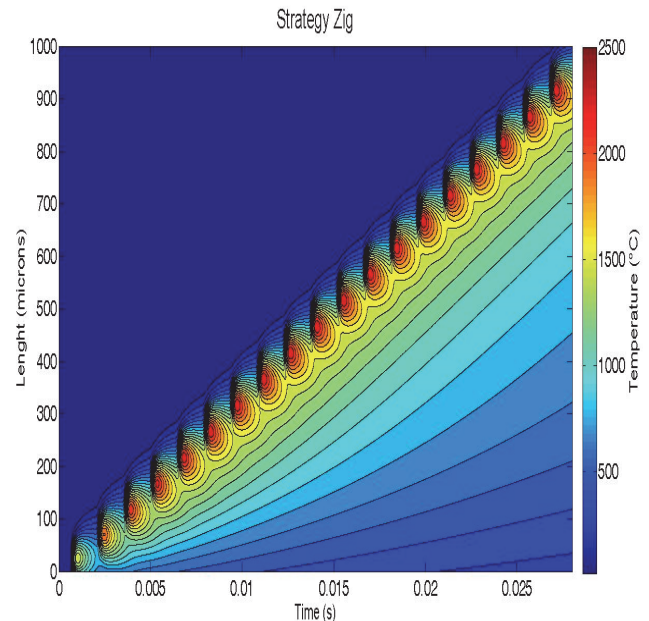


Fig. 11: Temperature map of the reference strategy

Unfortunately, these maps are not very practical. The maximum temperature evolutions are developed from these maps to have two-dimensional graphics.

Evolution of the maximum temperature

The evolution of the maximum temperature is obtain by keeping the maximum temperature at any time (see Fig. 12). These graphics allow to compare machining strategies more easily.

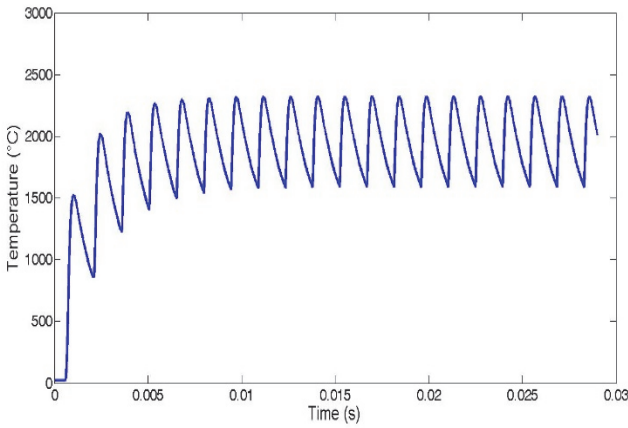


Fig. 12: Maximum temperature evolution of the reference strategy

4 RESULTS AND DISCUSSION

4.1 Trajectories comparison

The approach described in §3.2 is applied for the three paths at the depth of 30 μm for the three strategies. The temperature maps in the Fig. 13 allows to compare visually the three trajectories on the path 1. The accumulation of temperature in Zig-Zag trajectory is more important than for the other ones.

The temperature accumulation is around 1200 °C with contour strategy and around 1700 °C with Zig-Zag strategy.

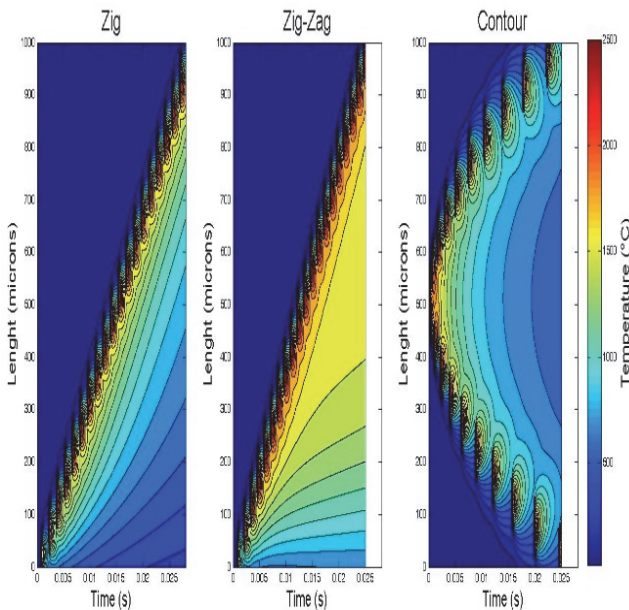


Fig. 13: Temperature maps on the path 1 for the three strategies

The heating time of the Zig strategy is more important as the others (Tab. 3). But the hot spots of Zig-Zag and contour parallel could be higher than the reference. The calculation of the heating time is the ratio between the scan velocity and the covered distance.

Tab. 3: Heating time for the three strategies

	ZIG	ZIG - ZAG	CONTOUR
Time (s)	0.0288	0.025	0.025

The evolution of the maximum temperature permits to detect hot spots and to compare their temperature.

The evolutions of the maximum temperature are shown on Fig. 14, Fig. 15 and Fig. 16. The heating time with Zig trajectory is longer than the others trajectories (see Tab. 1)

On path 1 (Fig. 14) localized on the middle of the pocket, maximum temperature of the contour parallel strategy is the lowest (cf. Tab. 4).

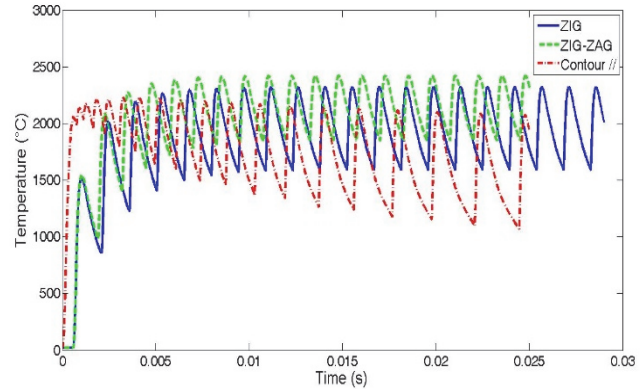


Fig. 14: Evolution of the maximum temperature on path 1

On path 2 (Fig. 15) localized on the corner of the pocket, contour's peak temperature is the highest. However, this temperature is not a hot spot because it is inferior to the maximum temperature on path 1.

The laser meet only once the path in Zig-Zag and contour strategies, while it crosses several times the path in the reference strategy. The evolution of Zig-Zag and contour parallel strategies are similar with an important peak because the temperature accumulation is more important on this path to these strategies.

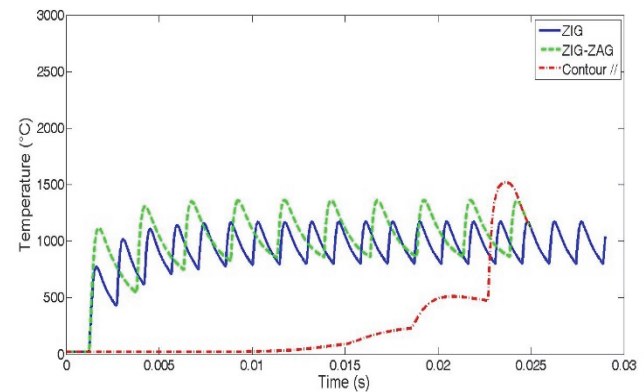


Fig. 15: Evolution of the maximum temperature on path 2

Finally on the path 3 (Fig. 16), the maximum temperature peak of the Zig-Zag strategy is the highest. The peak of the contour parallel strategy is higher than the reference trajectory (around 350°C) but it is not a hot spot. Indeed, the temperature peak in Zig strategy is superior on the path 1.

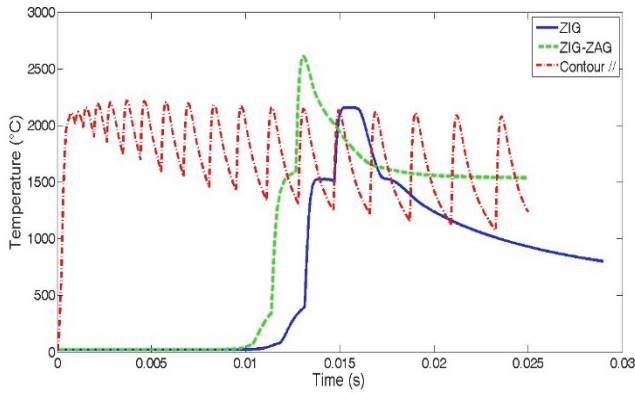


Fig. 16: Evolution of the maximum temperature on path 3

The Tab. 4 shows the different peaks of maximum temperature for each trajectory and on each path.

Tab. 4: Comparison hot spots for different trajectories (results in °C)

	ZIG	ZIG – ZAG	CONTOUR
Path 1	2321	2419	2224
Path 2	1170	1361	1518
Path 3	2158	2609	2216
Max.	2321	2609	2224

The peak temperature with Zig-Zag trajectory is the hottest point. This strategy must be avoided because the material removal rate may not be constant. The maximum temperature of the contour trajectory seems to be a little inferior for the hottest point (path 1) that the reference. But on the others paths, the maximum temperature of the contour parallel is higher than reference but less raise than this one path 1. The machining time of the contour parallel is less important than the time of the reference strategy

4.2 Comparison island size

In a second time, the model is modified by adding a square island in the centre of the pocket (Fig. 17). Two island sizes were considered 0.01 mm² and 0.04 mm².

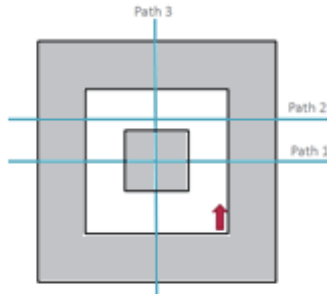


Fig. 17: Pocket with island and paths definition

As the contour parallel give the best result without island, numerical simulations are realised with the reference strategy and contour parallel strategy. These results are compared with the solution without island. The final results are exposed in Fig. 18.

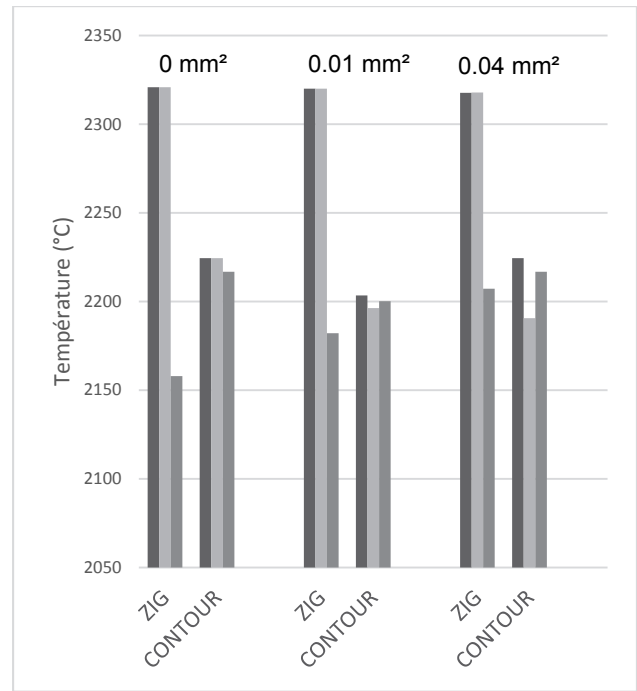


Fig. 18: Influence the island's size

The path 2 is modified in order to see influence of the island size. This path is parallel with path 1 and to the island along to visualize the laser behaviour to the bifurcation (see Fig. 17).

This graphic shows that the maximum temperature of the reference is the highest on the path 1. The temperature of the contour parallel strategy is a little less hot than the maximum of the reference. The maximum temperatures of the contour trajectory are near on the three paths. By contrast, a maximum temperature of the Zig trajectory is inferior (path 3) than the others.

The Tab. 5 illustrated maximum temperature comparison against for maximum temperature in the reference strategy and machining time. The value of the hottest spot, on the path 1 with the Zig strategy, is equal of 100%.

The maximum temperature of contour parallel strategy is near than maximum value but this is stable.

The heating time of the contour parallel strategy is always more interesting than the reference.

Tab. 5: Maximal temperature comparison in % and machining time (s)

	Zig		Contour		Zig		Contour	
	0 mm ²		0.01 mm ²		0.04 mm ²			
Path 1	100	95.85	99.97	94.94	99.86	95.85		
Path 2	100	95.85	99.97	94.63	99.87	94.39		
Path 3	92.98	95.51	94.02	94.80	95.11	95.51		
Time	0.029	0.025	0.029	0.025	0.029	0.025		

5 CONCLUSION

Thermal models were developed with the finite element software Abaqus v6.11 to model laser heating.

First, a thermal model with a moving heat source on a Y-TZP block was developed. The source was modelled with no overlap to take into account the repetition rate and pulse duration. The simulation results were validated with the analytical solution of Rosenthal.

Then, another model was created to compare several laser strategies to machine a pocket. Three strategies were implemented in the model: Zig (the reference), Zig-Zag and contour parallel. A method based on the temperature map along a path was developed to compare hot spots and machining time of these strategies.

The Zig-Zag trajectory is to avoid because there are more hot spots and at higher temperature than the reference strategy (Zig).

By contrast, hot spots with contour parallel are lower than the maximum of the reference. The maximum temperatures of the contour parallel are near. The heating time for contour parallel and Zig-Zag is smaller than the time for the Zig strategy.

Finally, an island of two different sizes was implemented in pocket model. In this model, the trajectories Zig and contour parallel were compared. The contour parallel strategy remains more interesting than the Zig strategy. Indeed, the hot spots are again lower than hot spots of Zig trajectory. The heating time of the Zig strategy is more important than the contour parallel strategy.

In summary, the contour parallel strategy is a strategy faster than the Zig strategy. The maximum temperatures of this strategy are near.

By contrast, the Zig strategy causes a maximum temperature on a path who is lower than the two others.

The heating time of the contour parallel is interesting in the current socioeconomic context.

In perspective, the model must take into account the crater formation (evaporation and melt ejection) and the dependence of the material properties with temperature.

The experimental experiments must be realised to compare the roughness and geometric tolerances.

This modeling approach could be used to other techniques as cladding technique and selective laser melting of metals.

6 NOMENCLATURE

Q laser power (W)
 v scanning spot (m/s)
 Ud the degree of overlap (%)
 ρ density (kg/m³)
 α diffusivity (m²/s)

λ conductivity (W/m²K)
 c_p specific heat (J/kgK)
 T temperature (°C)
 r distance between point heat source and point target (m)
 t time (s)
 (x,y,z) fixed coordinate system
 (ξ,y,z) moving coordinate system

7 REFERENCES

- [Filsler 2001] Filsler, F.T. Direct Ceramic Machining of ceramic dental restorations. Diss ETH No. 14088. Zurich: Swiss federal institute of technology Zurich, 2001.
- [Denry 2008] Denry, I. and Kelly, J.R., State of the art of zirconia for dental applications. Dental Materials; March 2008, Vol. 24, Issue 3, pp 299-307.
- [Vora 2013] Vora, H.D., Santhananakrishan, S., Harimkar, S.P., Boetcher, S.K.S. and Dahotre, N.B, One-dimensional multipulse laser machining of structural alumina: evolution of surface topography. The International Journal of Advanced Manufacturing Technology, September 2013, Vol. 68, Issue 1-4, pp 69-83.
- [Carslaw 1959] Carslaw, H.S., and Jaeger, J.C., Conduction of heat in solids. Oxford at the Clarendon press 1959.
- [Darmadi 2011] Darmadi, D., Norrish, J., and Tieu, A.K. Analytic and Finite Element Solutions for Temperature Profiles in Welding using Varied Heat Source Models. World Academy of Science, Engineering and Technology, 81, pp 154-162.
- [Piekarska 2010] Piekarska, W., Kubiak, M. and Saternus, Z. Application of Abaqus to analysis of the temperature field in elements heated by moving heat sources. Archive of foundry engineering, July 2010, Vol. 10, Issue 4/2010, pp 177-182, ISSN 18973310
- [Kaldos 2004] Kaldos, A., Pieper, H.J., Wolf, E., Krause, M. Laser machining in die making—a modern rapid tooling process. Journal of Materials Processing Technology, November 2004, Vol. 155-156, pp 1815-1820.
- [Heyl 2001] Heyl, P., Thomas Olschewski, T., and Wijnaendts, R.W., Manufacturing of 3D structures for micro-tools using laser ablation. Microelectronic Engineering, September 2001, Vol. 57-58, pp 775-780.